INVESTIGATION OF VSTOL AIRCRAFT ENGINE SURGE DUE TO GROUND VORTEX INGESTION

J. Lepicovsky

Institute of Thermomechanics, AS CR
Prague, Czech Republic

A. A. duPont

duPont Aerospace Company
Manchester Center, Vermont, U.S.A.

Keywords: VSTOL aircraft, engine surge, vortex ingestion, ground vortex

ABSTRACT

An investigation of flow instabilities in the inlet ducts of a two-engine vertical takeoff and landing aircraft DP-1C is described in this paper. The engines stalled during run ups while the aircraft was operated on the ground. These pop stalls occurred at relatively low power levels, sometimes as low as 60% of the engine full speed. The main focus of the paper is on instrumentation of the aircraft intake ducts and on high speed recording the flow instabilities during the engine rotating stall and surge events. The recorded data sets show the history of speeds of both engines and the associated history of pressure changes recorded by six pressure transducers installed in both inlet ducts. Analysis of recorded unsteady pressure data indicated that engine stalls were evoked by a sudden ingestion of a vortex generated between the two streams moving in the opposite directions: hot gas flow close to the ground streaming outbound from the main nozzle and inbound flow above in the engine inlets. The engine stall problem was eventually resolved by modifying the overall flow pattern at the engine intake lips by deploying a suitably shaped double scoop flow deflector.

NOMENCLATURE

N1 [%] engine speed

t   [s]   time

π_x [1] pressure ratio

INTRODUCTION

The duPont Aerospace DP-1C aircraft was a 53% scale prototype demonstrator for a fixed-wing vertical/short-takeoff-and-landing (VSTOL) small transport airplane (Figs. 1 and 2). The aircraft was intended for high subsonic speeds with a uniquely designed jet vectored thrust allowing VSTOL capability (duPont & Reuss, 2003). Two Pratt & Whitney Canada 530A turbofan engines powered the aircraft. The engines were located side-by-side in the front fuselage past inlet ducts. Engine exit nozzle flows were separately vectored for 90 deg by pivoted airfoil cascades located in the fuselage center of gravity to facilitate transition from the

vertical to the horizontal flight regimes and vice versa (Fig. 3).

Figure 1: Aircraft DP-1C (side view)

Figure 2: Aircraft DP-1C (front view)
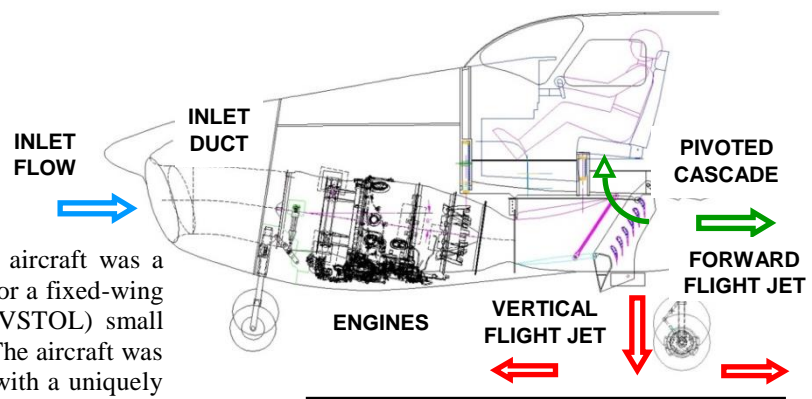
Figure 3: Thrust vectoring device

Initial tests of the thrust vectoring device were performed on a mesh platform elevated 3 m above the ground (Fig. 4). However, later when the aircraft was tested on the ground the engines stalled during run ups. These pop stalls occurred

even at relatively low power levels, sometimes as low as *60%* of the engine full speed. Inability to run the engines up to the full speed level was attributed to in-ground effects associated with either by ingestion of hot gases streaming forward from the main exit nozzle (see Fig. 3) or by ingestion of ground vortices. Other possible causes for the ground proximity stalls, like vortices generated by the nose undercarriage excited by the forward flow from the exit nozzles or double inlet mutual flow instability, were also considered (duPont, 2007). In order to understand this problem a decision was made to carry out detail unsteady pressure measurements in engine inlets.

Figure 4: Elevate test platform

INSTRUMENTATION

The main focus of the paper is on instrumentation of the aircraft intake ducts and on recording the flow instabilities during the engine rotating stall and surge events. The task was to devise an approach requiring only minimum modifications of the inlet ducts, allowing easy installations of the pressure transducers allowing to anticipated frequent swapping of the measurement stations, and above all protecting the sensitive transducer from damage. Miniature pressure transducers were packaged into modules that allowed easy installation, simple and reliable electric and pneumatic connections, and maximum transducer protection for mishandling and harsh environment damage. A view into the open transducer package is shown in Fig. 5; here "**A**" is the miniature pressure transducer, "**B**" is the electric connector, "**C**" is the pneumatic connector for transducer back pressure, "**D**" is the pneumatic connector for an ordinary static pressure tap, "**E**" is the box base with insertion boss, and "**F**" is the box cover (Lepicovsky, 2008).

A view of instrumented engine intakes with the aircraft nose cowling removed is shown in Fig.6. In this figure, "**A**" indicates the mounted transducer boxes and "**B**" and "**C**" show access ports on the left and right engine intakes, respectively. A detail view of installed pressure boxes is shown in Fig. 7. Finally, there is a view into the instrumented left engine inlet in Fig. 8. The insert in this figure spots two pressure ports in the insertion boss. The port

labeled "**U**" is directly connected to the high frequency pressure transducer inside the box, whereas the port "**S**" is connected by long tubing to a low frequency pressure transducer for detecting average flow wall static pressures.

The layout of the experimental arrangement is shown in Fig. 9, including the labels of individual components. An overall view of the test site is illustrated in Fig. 10. The data acquisition unit was located on board the aircraft and was connected to the main computer in the control station via a fiber optics link. A view of the onboard unit, located behind the pilot seat, is presented in Fig. 11.
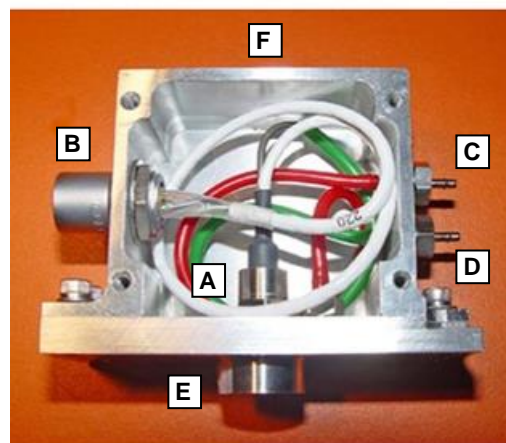
Figure 5: View into transducer package
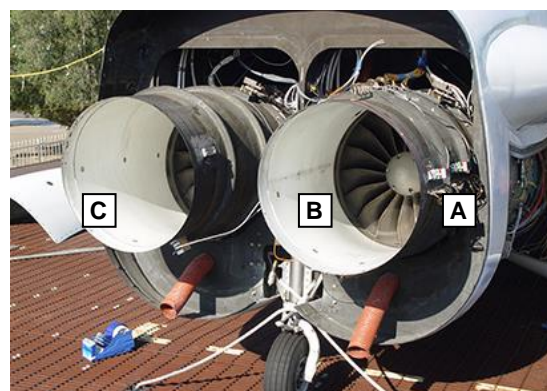
Figure 6: Instrumented engine intakes

Figure 7: Detail view of intake instrumentation
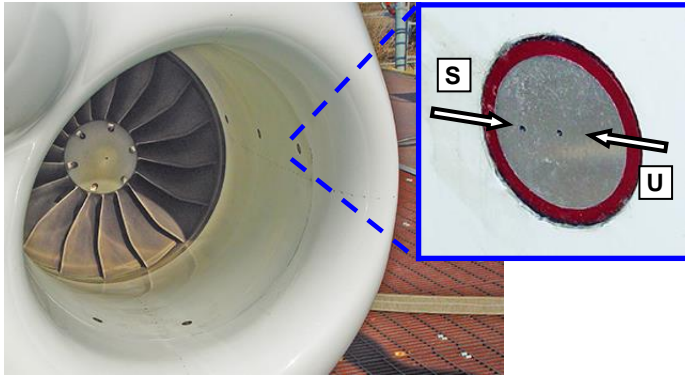
Figure 8: View of instrumented access ports

Figure 11: On-board main data acquisition unit
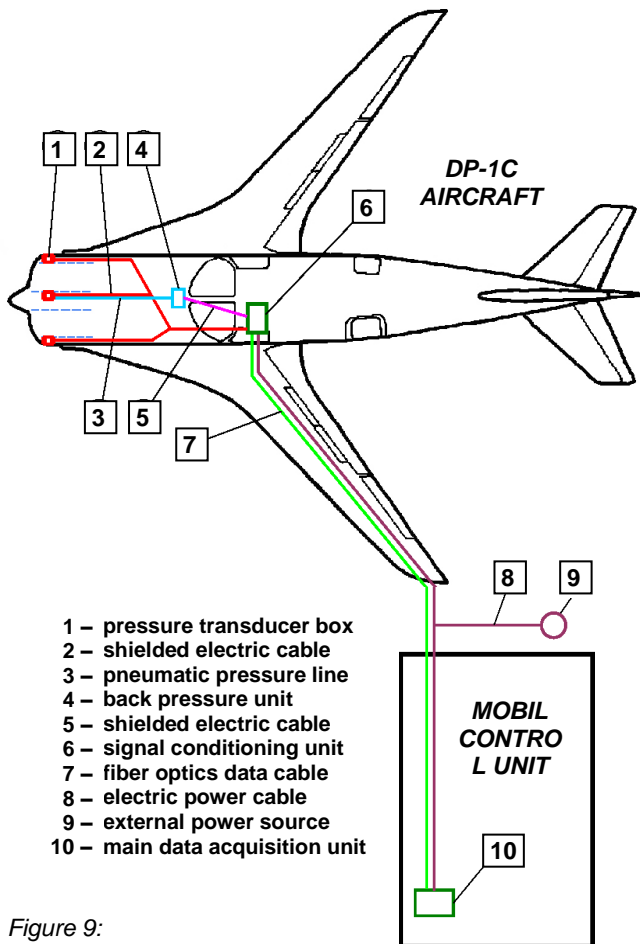
Figure 9:
Schema of experiental layout

1 – pressure transducer box
2 – shielded electric cable
3 – pneumatic pressure line
4 – back pressure unit
5 – shielded electric cable
6 – signal conditioning unit
7 – fiber optics data cable
8 – electric power cable
9 – external power source
10 – main data acquisition unit

EXPERIMENTAL RESULTS

There were no pop stalls recorded or observed when aircraft was powered while on the elevated platform, and engines thus ran-up to the full speed. As mentioned above, when aircraft was powered on the ground the engines stalled at power levels above 60% which was manifested by extremely loud bangs. It was recognized from the beginning that the main culprit for stalling was either the ingestion of vortex structures generated around the front part of the fuselage or excited flow instability in the inlet ducts. In order to resolve this question everal test runs were performed with fully instrumented inlet ducts.

The recorded data sets show the history of speeds of both engines and the associated history of pressure changes recorded by six pressure transducers in both inlet ducts. The following figures, Fig. 12 through Fig. 15, depict the same event of the left engine stall, albeit in different time resolutions. As seen in Fig. 12, both engines accelerated from about *60%* to *70%* speed, the left engine (red curve) being slightly faster. At about *72%* speed, the left engine stalled (small dip in the red speed curve, arrow *A*), while the right engine was running smoothly.

Figure 10:
Mobil control unit and elevated test platform
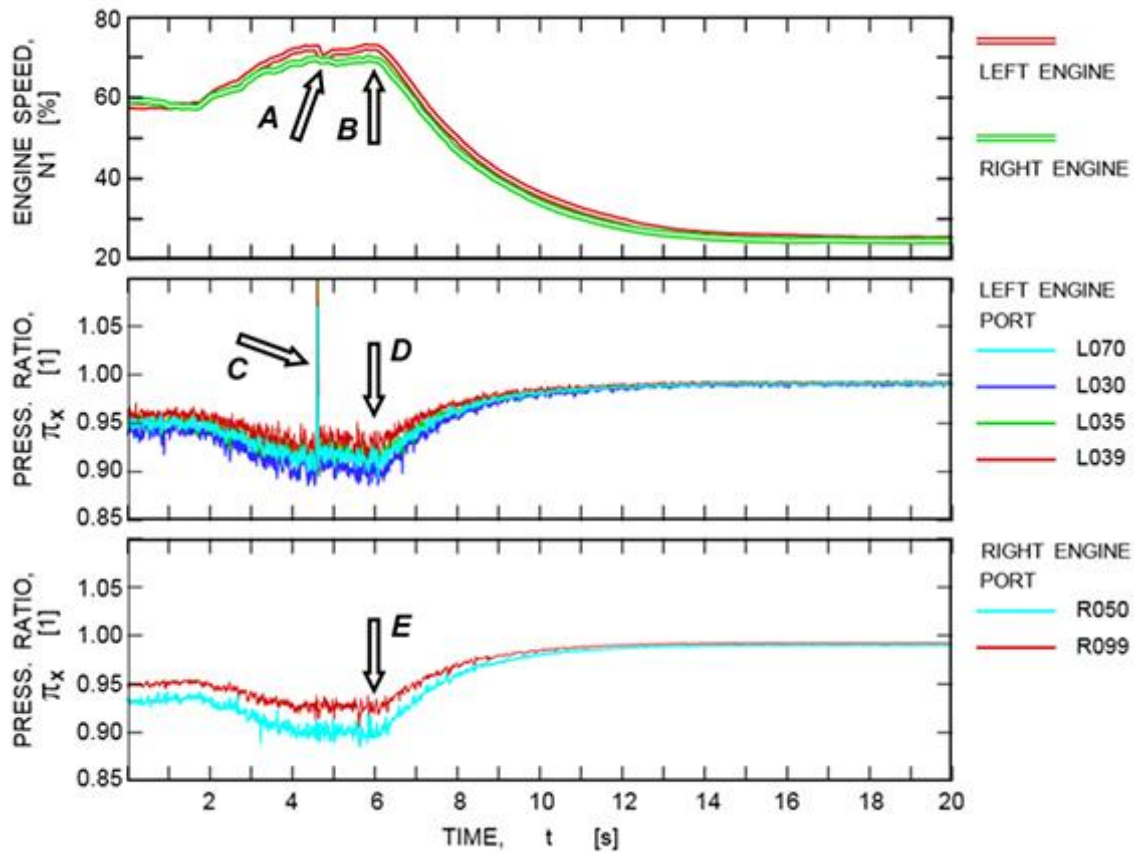
Figure 12: Left engine single stall event (20.0 s segment)

Approximately *1.5* seconds after the left engine stall occurred the pilot throttled back both engines (arrow *B*), and the engines decelerated to *25%* speed. As seen in the middle chart of the same figure, wall pressures in the left inlet duct were initially decreasing at the beginning of the record as the engine accelerated, and then a sudden pressure spike (arrow *C*) appeared indicating the engine stall. Wall pressure traces in the right inlet duct (the bottom chart) do not exhibit a pressure spike, which indicates no stalling of the right engine. After the engines were throttled down (arrows *D* and *E*), the wall pressures in both inlet ducts increased to nearly an ambient pressure level as the both engines were at idle.

A sudden drop in the speed of the left engine during the stall period is more visible in Fig. 13 (arrow *A*, red line). The fan velocity reaches its local minimum in about *0.2 s* from the instant of the stall start, then the speed increases rapidly for about *0.3 s*, and finally after additional *0.9 s* the fan speed is back at its pre-stall level.

A sequence of pressure changes in the inlet duct can be clearly detected in Fig. 14. The interval depicted in this plot is reduced to *60 ms*. It is difficult to reconstruct the flow behavior based solely on the wall static pressure data (total pressure or velocity data would have been more definitive); nevertheless, the following scenario is most probable. Ahead of the pressure surge the

pressure level in front of the fan is slightly higher than that at the inlet lip which indicates undisturbed flow through a mildly diffusing inlet duct (red line versus blue line).

Once the engine stalls, a pressure burst (arrow *A*) propagates from the fan face (port *L039*, red line, #1) through the inlet duct (port *L035*, green line, #2) towards the inlet lip (ports *L030* and *L070*, dark and light blue lines, #3). The pressure level in the entire duct increases significantly, and then for a short period the flow in the inlet duct stops (all pressures in the inlet duct are equal; there is no time delay among the data lines). While there is a little flow in the inlet duct, the pressure level in the entire duct is uniformly dropping (arrow *B*). After that, the pressure level just in front of the fan increases again (red line, arrow *C*), whereas the pressures at the mid channel (green line) and at inlet lip (blue lines) are more or less steady (disregarding small very low frequency oscillations), and close to the ambient pressure level (arrow *D*). Such a static pressure distribution may indicate reverse flow in the inlet duct, which lasts for about *30 ms* (approximately *6* engine revolutions). Finally, the flow stops again (all pressures in the inlet duct are equal, all data lines collapse together), and inflow in the fan starts again (arrow *E*) as the engine resumes normal operation.

40
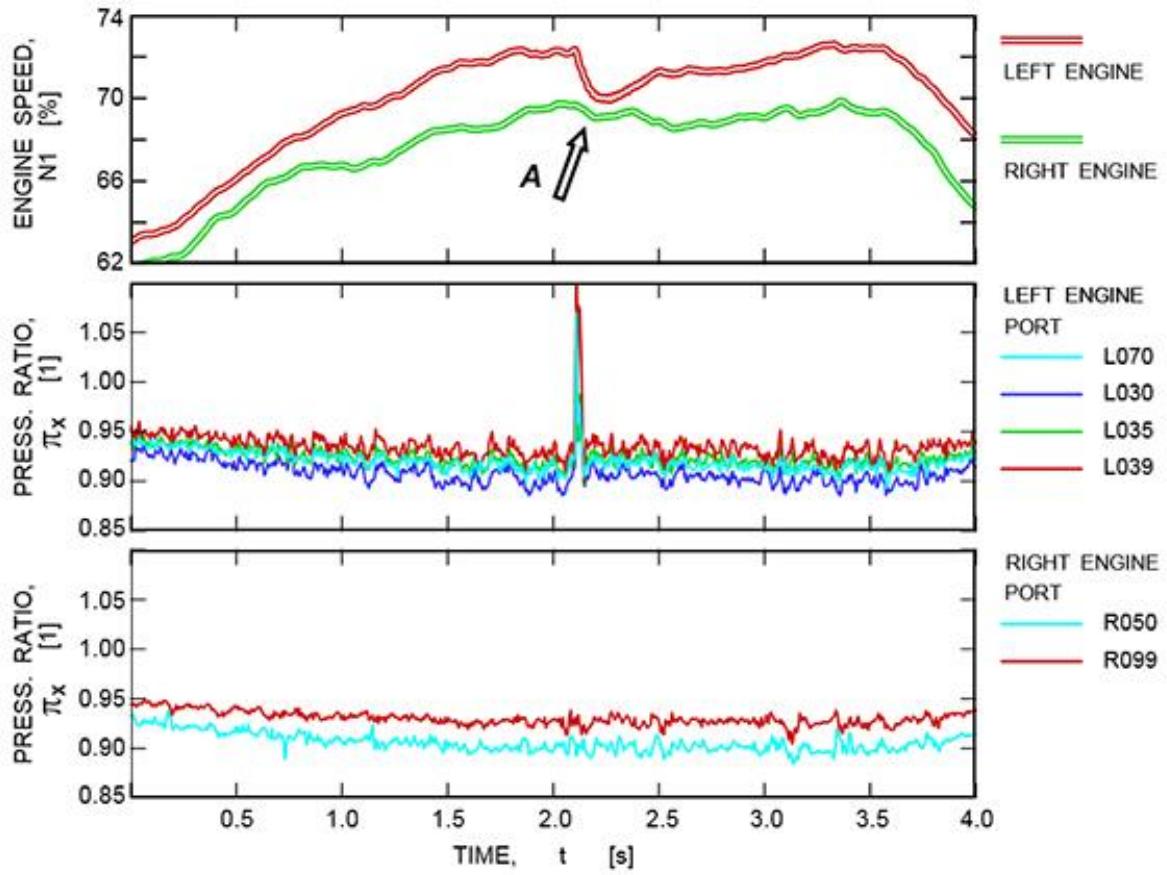
Figure 13: Left engine single stall event (4.0 s segment)
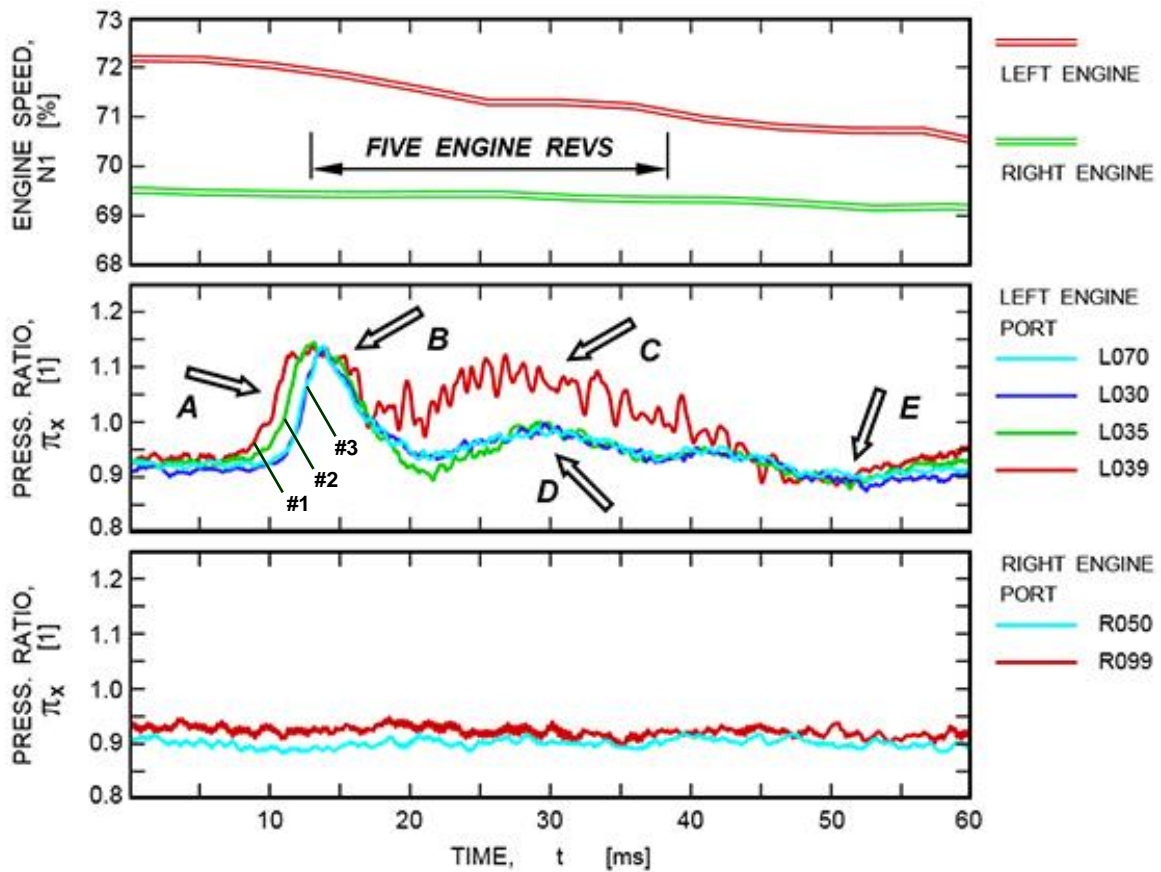
Figure 14: Left engine single stall event (0.06 s segment)

41

The propagation speed of the pressure burst can be determined reliably by measuring the time interval for the pressure burst to travel from one measurement port to another. As already indicated in Fig. 15, the pressure burst for a pressure level of $\pi_x = 1.05$ spreads from port *L039* (fan front face, #1) to port *L035* (mid inlet duct, #2) in *0.947 ms*, and it takes an additional *1.073 ms* for the burst to reach port *L030* (inlet lip, #3). The average propagation velocity of the pressure burst is about *289 m/s*. This is a propagation velocity relative to the inlet surface, not relative to the incoming flow; of course, a pressure disturbance propagates in air with the speed of sound, which in this case was about *349 m/s*, based on the measured total (ambient) temperature of *303 K*. It implies that the air inlet velocity could not be higher than *60 m/s*. In pre-stall operation was the inlet flow velocity about *135 m/s* for the relative engine speed of *72%*. Obviously, the pop stall occurrence had to decrease the inlet flow velocity significantly.

Finally, the segment of data as presented in Fig. 15 is shown once again in Fig. 16; however, this time unfiltered data are shown. As seen in this figure in the records for the right engine (bottom chart in the figure), the data sampling frequency was sufficiently high to distinguish blade potential flow fluctuations ahead of the engine fan (red line, port *R099*). As seen in this chart, effects of all *17* blades are clearly captured during one fan revolution.

It is worthwhile to note that the potential flow fluctuations evoked by the moving fan blades can be detected as far as at the inlet lip (blue line, port *R050*). However, the potential flow variations are not detected in the inlet duct of the left engine that underwent the stall event (mid chart in this figure). It indicates that the potential flow pattern during the stall period is in the inlet duct completely disrupted.

An interesting data set is shown in Fig. 17. During this test run, the left engine stalled twice in a row, with only *256 ms* separating the stalls, as depicted in this figure. The stall pressure bursts are labeled *Stall A* and *Stall B* for later identification. Surprisingly, *Stall B* occurred during the recovery phase of *Stall A* at a visibly lower engine speed than the one at the *Stall A* instant. This may indicate that engine stalls are not set off by continuous or a long time scale event, but by some sudden intermittent disturbance in the inlet flow. If, for example, the engine stall is set off by a ground vortex intrusion in the inlet, then in this case the pressure burst and outflow from the inlet generated by *Stall A* did not blow the ground vortex away from the inlet, but the vortex returned back in the inlet, set the *Stall B*, and then finally was blown away by the second burst (*Stall B*). It appears that after *Stall B*, the engine was recovering to normal operation, but was terminated by throttling both engines.

An important fact to be noticed in these figures is that there is no detected instability in the inlet duct wall static pressures prior to the arrival of pressure bursts caused by the engine stalls. It appears that the inlet disturbance which leads to engine stalls is not manifested by changes in the wall static pressure distribution of the inlet flow. Also, it should be mentioned that stalls of both engines at the same time were never recorded.

PROBLEM SOLVING

The facts stated above indicate that engine stalls were probably evoked by a sudden ingestion of a vortex generated between the two streams moving in opposite directions: outbound hot gas stream from the main nozzle close to the ground and inbound inlet flow above. At a certain velocity ratio of these two streams, which is a function of engine speed, the vortex reaches an intensity level at which the left or the right end of the vortex attaches to a firm surface (either ground or the surface of the aircraft) and the other end is swallowed by one of the aircraft inlets. Once the vortex enters the inlet duct a puff of hot air can be sucked through the vortex core into the engine. Because the vortex core size is significantly smaller than the inlet diameter, wall static pressures on the inlet inner walls are not or only very little affected by the vortex presence. Once the engine stalls, the outflow from the inlet pushes the vortex away and the engine resumes normal operation. Because the engines were always throttled down after the pilot heard the pop noise, it is difficult to predict what would happen next.

It appeared that a possible remedy might be modifications of the flow pattern ahead of the inlet lips (Saripalli et al., 1997). Extensive smoke and tufts flow visualization ahead of the aircraft inlets were carried out for several flow deflector configurations. A collar around the fuselage front part as shown in Fig. 18, proved not to be effective at all. On the other hand retractable double scoop flow deflector, hinged at the front fuselage under the inlet lips (Fig. 19, proved very successful.

Extensive smoke and tufts flow visualization around the engine inlets indicated significant changes in the overall flow pattern. Results of these tests are summarized in Figs. 20 through 23. In each figure a bundle of tufts attached to a long stick is encircled by a yellow oval for better visibility; next to it is a red arrow indicating the prevailing flow direction in a given station in front of the inlets. As seen in Fig. 20, for no deflector, the flow arrow points vertically from the ground directly into the inlets, which result in engine stalls.
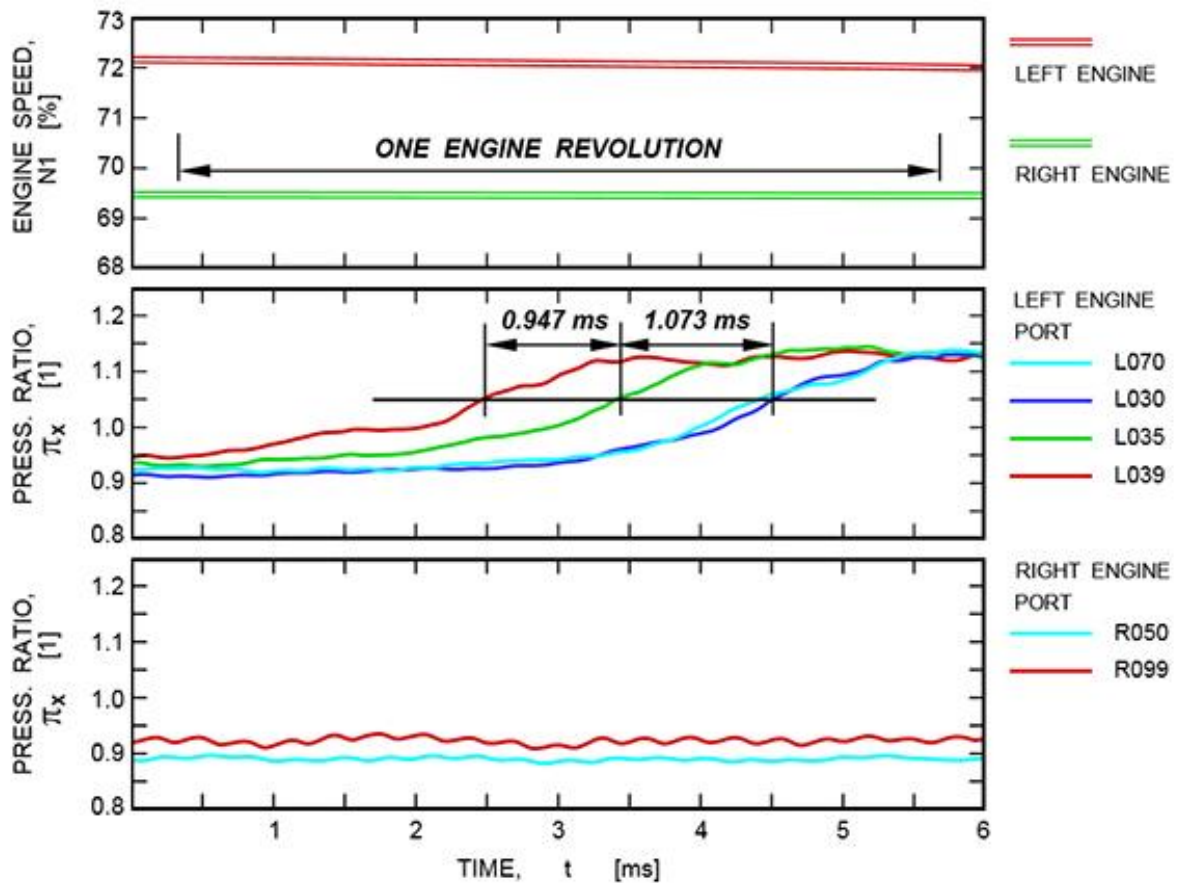
Figure 15: Left engine single stall event (0.006 s segment)
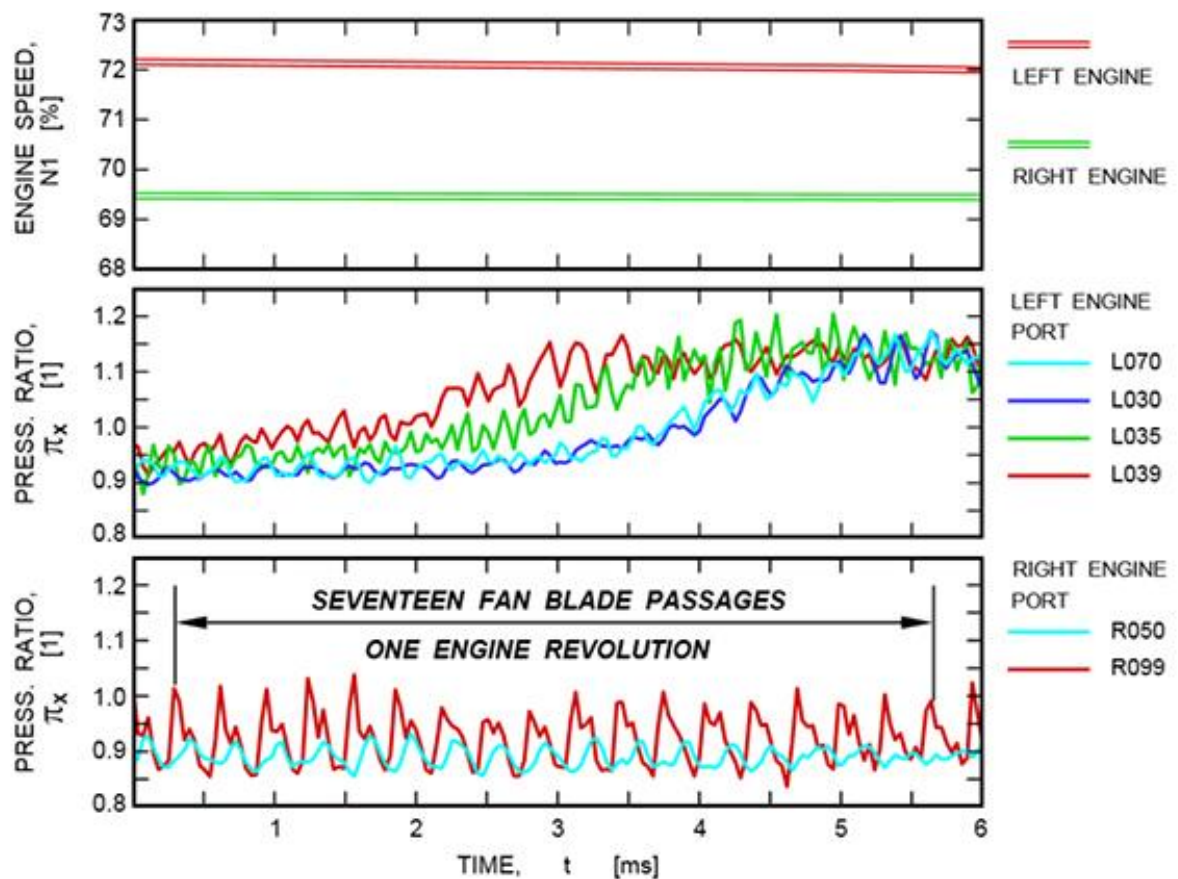
Figure 16: Left engine single stall event; unfiltred data (0.006 s segment)
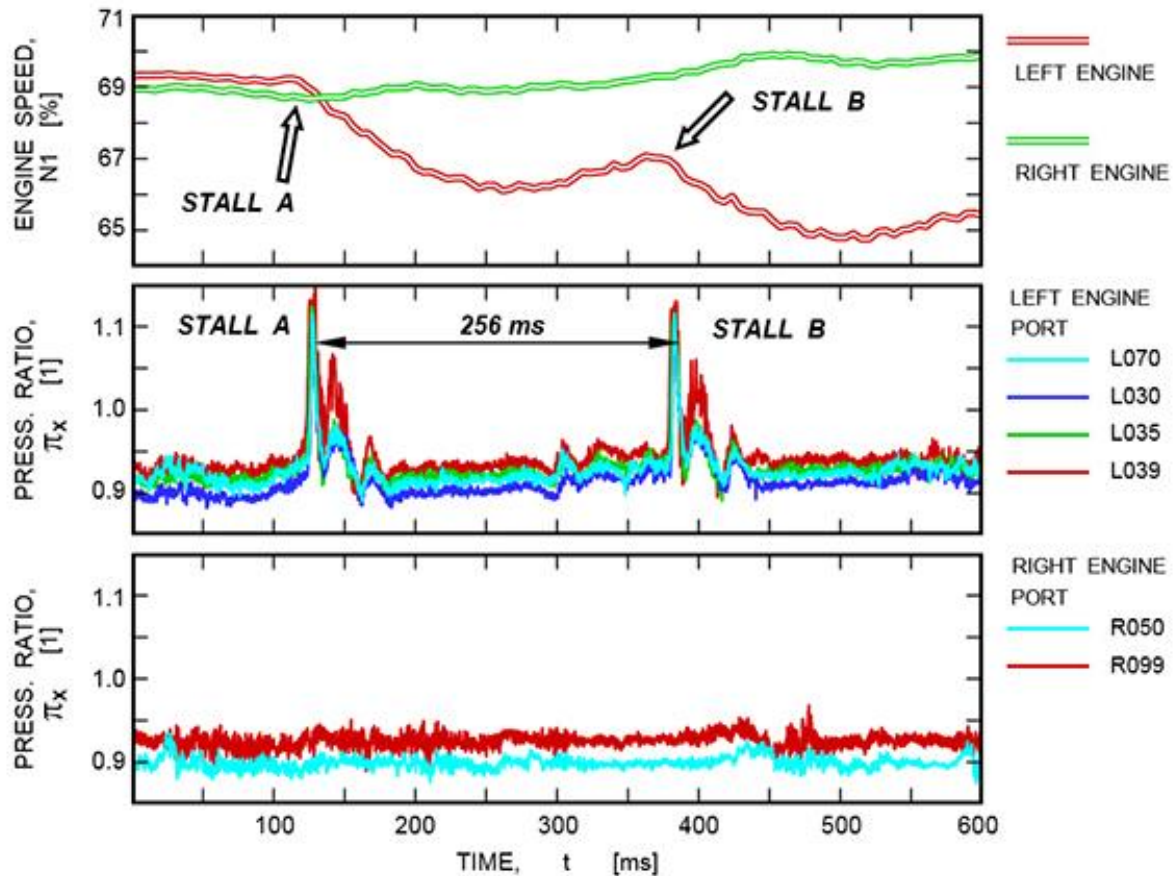
Figure 17: Left engine double stall event (0.6 s segment)

Figure 18: Collar flow deflector

Figure 19: Double scoop flow deflector

The situation is significantly different for the deployed scoop deflector. At the ground level (Fig. 21), there is a strong flow in the forward direction. It appears that at the inlet lower lip station (Fig. 22), the flow is turning towards the inlets. Finally, at the mid inlet station (Fig. 23) the flow rushes directly into the engine inlet.

As mentioned above, the deployed double scoop flow deflector eliminated engine stalls for the in-ground operation. A very good explanation of this fact is offered by Shmilovich & Yadlin (2006) who investigated the effects of tail wind strength on an engine inlet flow pattern.

The essence of there findings is shown in Fig. 24, which is reproduced from their paper. For a weak tail wind the boundary of an inlet flow capture area reaches the ground plane ahead of the inlet and the forward flow under the nacelle is "blocked" and the ground vortex is created (left sketch in Fig. 24). Similar effects appear while using thrust reversing to assist braking after landing (Motycka, 1976). On the other hand, strong tail wind detaches the capture area boundary from the ground, and the capture area encloses the engine inlet, which prevent the ground vortex formation (right sketch in Fig. 24).

Figure 20: Prevailing flow at ground level no flow deflector

Figure 22: Prevailing flow at inlet lip level;scoop flow deflector deployed

Figure 21: Prevailing flow at ground level; scoop flow deflector deployed

Figure 23: Prevailing flow at inlet mid level; scoop flow deflector deployed

It needs to be stated here that during the vertical take off the lift vertical jet impinges the ground and it spreads horizontally in all direction. Thus effectively it represents "tail wind" for the engine inlets. Deploying the hinged flow deflector (Fig. 19) creates a "flat convergent nozzle" under the engine inlets and effectively increases the "tail wind velocity" which precludes the ground vortex formation.
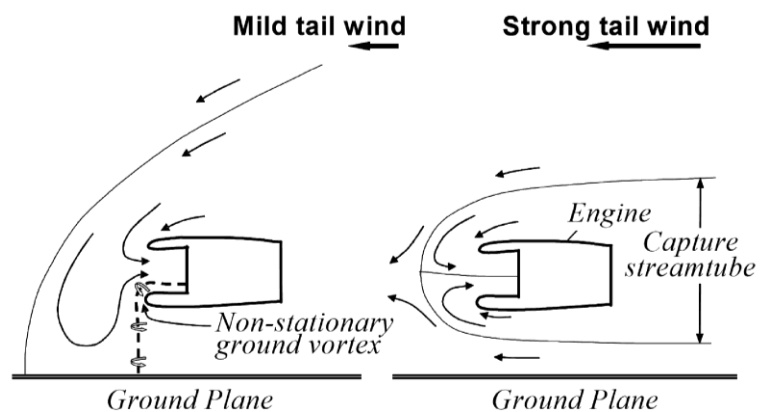
Figure 24: Effects of tail wind strength on ground vortex formation.

CONCLUSIONS

Extensive experimental investigations of flow instabilities in the inlet ducts of a two-engine vertical takeoff and landing aircraft DP-1C was carried out. An experimental approach was devised that required only minimum modifications of the inlet ducts, allowed easy installations of the high frequency pressure transducers, and secured excellent protection of the sensitive transducer for damages. Detailed analysis of experimental

indicated that engine stalls were evoked by a sudden ingestion of a vortex generated between the two streams moving in opposite directions: outbound hot gas stream from the main nozzle close to the ground and inbound inlet flow. The problem was resolved by employing a double scoop flow deflector hinged at the front fuselage under the inlet lips. Flow visualization experiments proved that the change in the inlet overall flow pattern, while the deflector was deployed, prevented the ground vortex formation

and thus the engine stall were avoided. It turned out that the deflector effects on ground vortex formation were similar to the effects of increased the "tail wind" speed as reported elsewhere in the open literature.

REFERENCES

[1] DuPont, A. A. & Reuss, R. P.; 2003. "Testing an Inlet for a Twin Engine VTOL Aircraft". Paper ISABE 2003-1112.

[2] DuPont, A. A.; 2007. "Tethered Hover of DP-1C Test Aircraft," Final report, ONR Contract no. N00014-07-C-0385.

[3] Lepicovsky, J.; 2008. "Investigation of Flow Instabilities in the Inlet Ducts of DP-1C VTOL Aircraft", Report NASA/CR -2008-215216.

[4] Motycka, D. L.; 1976. "Ground Vortex – Limit to Engine/Reverse Operation," Transaction of the ASME, Jour. of Engineering for Power, pp. 258-264.

[5] Saripalli, K. R.; Flood, J. D. & Moss, G. M.; 1997. "Inlet Hot Gas Ingestion (HGI) and Its Control in V/STOL Aircraft," AIAA Paper 975517.

[6] Schmilovich, A. & Yadlin. Y.; 2006. "Engine Ground Vortex Control", Paper AIAA 2006-3006